

1 **The potential role of sediment organic phosphorus in algal growth in a low**
2 **nutrient lake**

3 Zhaokui Ni^a, Shengrui Wang^{a, b, c*}, Jingjing, Cai^a, Hong Li^{d, e}, Alan Jenkins^d, Stephen
4 C. Maberly^f, Linda May^g

5

6 ^a Engineering Research Center of Ministry of Education on Groundwater Pollution
7 Control and Remediation, College of Water Sciences, Beijing Normal University,
8 Beijing 100875, China

9 ^b China Three Gorges University, College of Hydraulic&Environmental Engineering,
10 Yichang 443002, China

11 ^c Yunnan Key Laboratory of Pollution Process and Management of Plateau Lake-
12 Watershed, Kunming, Yunnan Province, 650034, China

13 ^d Centre for Ecology & Hydrology, Maclean Building, Benson Lane, Crowmarsh
14 Gifford, Wallingford, Oxfordshire OX10 8BB, UK

15 ^e Lancaster Environment Centre, University of Lancaster, Library Avenue, Lancaster
16 University, LA1 4YQ, UK

17 ^f Centre for Ecology & Hydrology, Lancaster Environment Centre, Library Avenue,
18 Lancaster LA1 4AP UK

19 ^g Centre for Ecology & Hydrology, Bush Estate, Penicuik, Midlothian EH26 0QB,
20 UK

21 **Abstract:** The role of sediment-bound organic phosphorus (P_o) as an additional
22 nutrient source is a component of internal P budgets in lake system that is usually
23 neglected. Here we examined the relative importance of sediment P_o to internal P load
24 and the role of bioavailable P_o in algal growth in Lake Erhai, China. Lake Erhai
25 sediment extractable P_o accounted for 11–43% (27% average) of extractable total P,
26 and bioavailable P_o accounted for 21–66% (40%) of P_o . The massive storage of
27 bioavailable P_o represents an important form of available P, essential to internal loads.
28 The bioavailable P_o includes mainly labile monoester P and diester P was identified
29 in the sequential extractions by H_2O , $NaHCO_3$, $NaOH$, and HCl . 40% of H_2O-P_o , 39%
30 of $NaHCO_3-P_o$, 43% of $NaOH-P_o$, and 56% of $HCl-P_o$ can be hydrolyzed to labile
31 monoester and diester P, suggesting that the bioavailability of P_o fractions was in
32 decreasing order as follows: $HCl-P_o > NaOH-P_o > H_2O-P_o > NaHCO_3-P_o$. It is
33 implied that traditional sequential fractionation of P_o might overestimate the
34 availability of labile P_o in sediments. Furthermore, analysis of the environmental
35 processes of bioavailable P_o showed that the stabler structure of dissolved organic
36 matter (DOM) alleviated the degradation and release of diester P, abundant alkaline
37 phosphatase due to higher algal biomass promoted the degradation of diester P. The
38 stability of DOM structure and the degradation of diester P might responsible for the
39 spatial differences of labile monoester P. The biogeochemical cycle of bioavailable P_o
40 replenishes available P pools in overlying water and further facilitate algal growth
41 during the algal blooms. Therefore, to control the algal blooms in Lake Erhai, an
42 effective action is urgently required to reduce the accumulation of P_o in sediments and

43 interrupt the supply cycle of bioavailable P_o to algal growth.

44

45 **Capsule abstract:** Sediment bioavailable P_o represents an important internal P load,
46 and the biogeochemical cycling of P_o can replenish additional nutrient source to
47 support algal growth

48

49 **Keywords:** Organic phosphorus; Bioavailability; Algal growth; Sediment

50

51 **1. Introduction**

52 Eutrophication and consequent harmful algal blooms are the major
53 environmental problems worldwide (Ngatia et al., 2017). In many aquatic ecosystems,
54 algal blooms are controlled by the availability of phosphorus (P) in the water column
55 (Ji et al., 2017). If a large amount of available P presented in the sediment, it can be
56 released into overlying water, accelerating eutrophication and delaying damaged
57 ecosystems recovery even after external inputs have been reduced. Numerous studies
58 have focused on investigating the size of the internally-available P pool and
59 evaluating the potential risk of eutrophication from sediment nutrient pools (Lei et al.,
60 2018; Chen et al., 2018; Wang et al., 2019). Sediment organic P (P_o) constitutes the
61 majority of P, and is critical to the biogeochemical cycling of P in many lakes
62 (Ahlgren et al., 2005; Ni et al., 2019; Baldwin, 2013; Ding et al., 2015). Although P_o is
63 abundant in sediment in some aquatic ecosystems, many studies of internal P loads

64 are still focused on the flux of phosphate release ([Shinohara et al., 2017](#); [Mandal et al.,](#)
65 [2015](#)). The contribution of bioavailable P_o is often neglected in estimations of internal
66 P load because of the complexity of P_o ([Worsfold et al., 2008](#); [Bai et al., 2009](#)). As a
67 result, sediment P load is largely underestimated by current assessment systems. An
68 improved understanding of the contribution of P_o to internal P load from sediment is
69 essential to formulate effective control strategies for lake eutrophication.

70 P_o consists mainly of sugar phosphates, phospholipids, nucleic acids, inositol
71 phosphates, and residual P ([Copetti et al., 2019](#)). The mechanism of adsorption of P_o
72 to lake sediments is similar to that of inorganic P (P_i) in sediments ([Worsfold et al.,](#)
73 [2008](#)). Phytoplankton and other organisms can take up phosphate released from
74 sediment via the enzymatic hydrolysis of P_o , and some species of phytoplankton can
75 even use small P_o molecules directly ([Huang et al., 2005](#); [Yue et al., 2014](#)). Evaluation
76 of the potential availability of P_o is usually dependent on geochemical fractionation
77 and enzymatic hydrolysis characteristics. Sequential extraction schemes have been
78 adopted by many scientists to determine the relative concentrations and fractions of P_o
79 ([Ruban et al., 1999](#)). Enzymatic hydrolysis has been used as a quantitative assessment
80 tool for hydrolysable P, since most P_o is hydrolyzed to orthophosphate before uptake
81 by phytoplankton and other organisms; thus hydrolysable P is a good indicator of the
82 bioavailability of P_o in sediment ([Bünemann, 2008](#)). These analytical techniques are
83 the powerful tools to determine the bioavailability of P_o and can improve our
84 understanding on the behavior and fate of P_o .

85 Lake Erhai is the second largest freshwater lake on the Yun–Gui Plateau of

86 China, and important tourist attraction and drinking water source for surrounding
87 cities such as Dali. At present, Lake Erhai is in the initial phase of eutrophication
88 (Wang et al., 2015). Long-term monitoring has shown that Lake Erhai has a relatively
89 high algal biomass, with average chlorophyll-*a* concentration of 14 $\mu\text{g L}^{-1}$ between
90 2003 and 2017 (Wang et al., 2015), exceeding the threshold level (or limit) set by the
91 Organisation for Economic Cooperation and Development (OECD) (1982) for
92 eutrophication. There have been frequent outbreaks of cyanobacterial blooms
93 observed in some part of the lake each year, especially in 2013 when almost 80% of
94 the lake area was affected. However, Lake Erhai contains relatively clean water, with
95 mean concentrations of total P, total dissolved P (TDP), and soluble reactive P (SRP)
96 of 20, 9.5, and 3.8 $\mu\text{g L}^{-1}$ from 2003 to 2017, respectively (Wang et al., 2015). Lake
97 Erhai is characterized by a high sediment P content, with total P contents ranging
98 from 419 to 1108 mg kg^{-1} (904 mg kg^{-1} average) (Zhao et al., 2013; Ni and Wang,
99 2015). As external P loads have significantly decreased in recent years, the release of
100 internal P accumulated in sediments has become an important source of P. Thus,
101 whether the release of P from sediments is sufficient to support high algal biomass
102 and the formation of algal blooms is a key research area that needs to be addressed.

103 Lake Erhai is a potentially P-limited lake (Yu et al., 2014). Previous studies have
104 focus mostly on the role of flux of inorganic P (P_i) release on lake eutrophication (Liu
105 et al 2015). However, little research has reported contribution of P_o to internal P load,
106 especially the impact mechanism of bioavailable P_o and the major classes of organic
107 molecules on algal growth. Assessing the contribution of P_o to internal P load and

108 potential role of bioavailable P_o on algal growth are therefore essential to understand
109 the fate of P_o . Accordingly, the main objectives of this study are to (1) investigate the
110 relative importance of P_o to internal P loads by sequential extraction, (2) characterize
111 the bioavailable P_o and the major classes of organic molecules using phosphatase
112 hydrolysis, and (3) examine the environmental processes of bioavailable P_o and its
113 potential role in algal growth.

114

115 **2. Materials and methods**

116 *2.1. Study Area*

117 Lake Erhai is adjacent to the suburbs of Dali City in Yunnan Province. It has an
118 area of 256 km², a mean depth of 10.5 m, and a volume of 27×10^8 m³. It supplies
119 drinking water and supports the socioeconomic development of Dali City. The lake is
120 at a high altitude (1972 m), located in an area with a subtropical monsoon climate,
121 and has an annual temperature range of 5 °C–15 °C. The average water residence time
122 is approximately 2.75 years. Topographically, the bottom of Lake Erhai can be
123 divided into three parts, namely the northern (sampling sites N1, N2, N3 and N4),
124 middle (sampling sites M1, M2, M3, M4 and M5), and southern (sampling sites S1,
125 S2, S3, S4 and S5) areas (Fig. 1). The northern part receives pollutants from
126 agricultural sources via three major rivers (Yongan, Miju, and Luoshi), with a mean
127 depth of 9 m. The middle part has no aquatic plant life, and receives relatively low
128 levels of pollutants, with a mean depth of 14 m. The southern part receives pollutants

129 mainly from domestic sources within the Dali administrative area, with a mean depth
130 of 7 m. Aquatic plants have been disappeared from the southern area since 2003, with
131 debris deposited onto the surface sediments.

132

133 *2.2. Sample collection and procedure*

134 Fourteen surface sediment samples (0–5 cm) were collected from the fourteen
135 sampling sites listed above using a columnar sampler (HL–CN, Xihuayi Technology,
136 Beijing, China) in September 2013. The sampling time represents a high–risk period
137 for the decline in water quality and the presence of algal blooms in Lake Erhai.
138 Overlying water samples were also collected from each sediment sampling site.

139 Sediment samples were stored in airtight plastic bags, and transported to the
140 laboratory in the dark at 4 °C. The samples were freeze–dried, ground to a powder,
141 and then passed through a 100 mesh sieve to ensure homogeneity prior to analysis.

142

143 *2.3. Analytical methods*

144 *2.3.1. Physicochemical analysis*

145 The organic matter (OM) content of the sediment samples was determined using
146 the K₂CrO₄ external heating method using 0.3 g of dried sediment ([Nanjing Institute
147 of Soil, Chinese Academic of Science, 1978](#)). Chlorophyll–*a* concentrations were
148 determined using a hot–ethanol extraction method ([Lorenzen, 1967](#)).

149

150 *2.3.2. Sequential fractionation of sediment P*

151 Sediment total P and its fractions (P_o , P_i) were extracted sequentially using the
152 modified method of He et al., (2004) and Zhu et al (2013), which can rapidly detect P_i
153 and P_o fractions, and produces P_o fractions that are suitable for subsequent enzymatic
154 hydrolysis. This method classifies P into four different categories: H_2O -P, $NaHCO_3$ -P,
155 $NaOH$ -P and HCl -P. Briefly, 1.0 g of dry sediment was extracted with 25 mL of
156 deionized water at 25 °C for 2 h. Then centrifuged at 10,000 g for 15 min and the
157 supernatant were passed through a 0.45 μm glass fibrefilter (Whatman, UK). Using
158 the same procedure, residues were then sequentially extracted with 0.5 mol L^{-1}
159 $NaHCO_3$ (pH 8.5), 0.1 mol L^{-1} $NaOH$, and 1 mol L^{-1} HCl for 16 h each to separate
160 the $NaHCO_3$, $NaOH$, and HCl fractions. In order to reduce contamination of
161 subsequent extracts by residual extractant and P in the pellet, after $NaHCO_3$ and
162 $NaOH$ extraction, residues were washed with 5 mL of deionized water, and the
163 supernatant was discarded after centrifugation. Total P and P_i of each fraction were
164 determined, respectively. P_o in each fraction was obtained using total P in each
165 fraction minus the corresponding P_i .

166 The pH of $NaHCO_3$, $NaOH$ and HCl extractions was adjusted so as to avoid
167 effect of pH on the enzymatic activity. The pH of the $NaHCO_3$ and $NaOH$ fractions
168 was adjusted to 7.0. The pH was adjusted to 5.15 in order to prevent HCl fractions
169 from precipitating after pH adjustment.

170

171 *2.3.3. Enzymes, buffers, and assay procedures*

172 Alkaline phosphatase (APase) and phosphodiesterase (PDEase) are widespread
173 enzymes in the water and sediment and play a key role in the biogeochemical cycling
174 of P (Hakulinen et al., 2005; Zhou et al., 2008 and 2002). APase and PDEase were
175 selected to characterize the bioavailability of P_o in the sediment, namely labile
176 monoester P and diester P.

177 For the hydrolase selection, preparation and combination, we used APase that
178 originated from bovine intestinal mucosa (EC 3.1.3.1, Type I–S, solid activity: 28 U
179 mg^{-1}), and PDEase that was derived from *Crotalus atrox* (EC 3.1.4.1, type I, solid
180 activity 0.02 U mg^{-1}). Both were purchased from Sigma–Aldrich Chemicals (St.
181 Louis, MO, USA). APase and PDEase were dissolved in Tris (hydroxymethyl)
182 aminomethane–HCl buffer (0.1 mol L^{-1} , pH 9) at concentrations of 1 and 0.02 U mL^{-1} ,
183 respectively. The solutions were stored in the dark for up to a week at 4 °C. To
184 characterize P_o more effectively, APase was used alone and PDEase was used in
185 combination with APase to achieve the complete hydrolysis of diester P. These
186 analyses were performed at pH 9 and at 37 °C.

187 For the assay procedure, we added MgCl_2 (0.002 mol L^{-1}) to the buffers as
188 enzyme activators. Trisodium citrate ($\text{Na}_3\text{C}_6\text{H}_5\text{O}_7 \cdot 2\text{H}_2\text{O}$) was added to prevent the
189 adsorption of released P_i by metal hydroxides during the assay. Prior to each assay, we
190 prepared mixtures of 5 mL of the H_2O fraction or pH adjusted extracts (NaHCO_3 ,
191 NaOH, and HCl fraction), 0.44 mL of APase (pH 9) or combination of APase and
192 PDEase (pH 9) in an appropriate buffer, and 0.05 mL of 0.68 mol L^{-1} trisodium citrate.
193 The mixtures were incubated for 16 h at 37 °C in a colorimetric tube (Monbet et al.,

194 [2007](#)).

195 The concentration of hydrolyzed P_o by each enzyme preparation was calculated
196 as the difference in P_i concentrations before and after incubation. Duplicate samples
197 and enzyme-free buffers were incubated simultaneously to identify and correct for
198 any non-enzymatic hydrolysis and/or matrix blank. Concentrations of phosphate were
199 measured using the molybdenum blue-ascorbic acid method. In order to avoid
200 enzyme precipitation, 1 mL of sodium dodecyl sulfate (2%) was added before
201 analysis.

202

203 *2.3.4. UV-visible absorbance spectroscopy*

204 The extracted solution was analyzed using a 1 cm quartz cuvette on a Hach
205 DR-5000 spectrophotometer at wavelengths ranging from 200–700 nm. E_2/E_3 and
206 A_{253}/A_{203} are the ratios absorbance at 250 nm to that at 365 nm, and at 253 nm to that
207 at 203 nm, respectively. Specific ultraviolet absorbances at 260 nm ($SUVA_{260}$) and
208 254 nm ($SUVA_{254}$) were calculated as 100 times the ratio of UV absorbance at 260
209 and 254 nm to the corresponding concentration of dissolved organic carbon.
210 Dissolved organic carbon was determined using a TOC analyzer (Shimadzu TOC-500,
211 Japan).

212

213 *2.3.5. Microorganism number analysis*

214 The total number of microorganisms was measured using the plate dilution
215 method ([Zhang et al., 2015](#)).

216

217 *2.4. Data analysis and quality control*

218 Data were analyzed and presented using SPSS 21 (IBM, Armonk, New York,
219 USA) and Origin 8.5 (OriginLab, USA). Duplicate field samples, spiked samples, and
220 blanks were used to control data quality. Triplicate measurements were conducted on
221 each sample and reported as arithmetic means. For each sample analysis, the variation
222 among replicates was less than 10%, and precision was almost 10% with a confidence
223 level of 95%.

224

225 **3. Results and Discussion**

226 *3.1. Risk of P_i and P_o releasing*

227 Extractable total P concentration in the surface sediments of Lake Erhai ranged
228 from 169 to 641 mg·kg⁻¹, with an average of 289 mg kg⁻¹. The concentrations of
229 extractable P_i and P_o fractions in the sediment are presented in Figure 2. The
230 concentration of extractable P_i ranged from 109 to 563 mg kg⁻¹ (218 mg·kg⁻¹ average),
231 which accounted for 57–88% of the extractable total P in the sediment. The P_i
232 fractions of the Lake Erhai sediments decreased in the following order: HCl- P_i >
233 NaOH- P_i > NaHCO₃- P_i > H₂O- P_i (Fig. 2a). The H₂O- P_i fraction was found in the
234 pore water of the sediments or loosely adsorbed onto the sediment particles (Zhou et
235 al., 2001), and accounted for 21–51% (39% average) of the total H₂O-P in the
236 sediment. The NaHCO₃- P_i contains slightly more labile adsorbed P, accounting for

237 36–87% (59% average) of the total $\text{NaHCO}_3\text{-P}$. The NaOH-P_i (Fe and Al
238 oxide-bound P) accounted for 48–92% (78% average) of the total NaOH-P . HCl-P_i
239 (calcium-bound P) accounted for 51–98% (86% average) of the total HCl-P . The
240 result of P_i fractions suggested that P_i in Lake Erhai sediments exists mainly in the
241 forms of HCl-P and NaOH-P . HCl-P is considered to be nonbioavailable and
242 difficult to release from sediment unless the environment is acidic ($\text{pH} < 6$) (Jin et al.,
243 2006; Kim et al., 2003). NaOH-P is a potential source of labile P that could be
244 released into overlying water when anoxic conditions prevail at the sediment–water
245 interface (Ting and Appan, 1996). Lake Erhai exhibited relatively stable pH and DO
246 concentrations in the bottom water from 1992 to 2014, with mean values that ranged
247 from 8.7–9.7 mg L^{-1} and 5.2–7.3 mg L^{-1} , respectively (Wang et al., 2015). Therefore,
248 the risk of P_i releasing from Lake Erhai sediments could be alleviated because of the
249 persistent aerobic state and stable pH value. This largely explains the reason why the
250 content of total P is high in Lake Erhai sediments (Zhao et al., 2013), but the flux of
251 SRP release is relatively low compared with the China’s five largest freshwater lakes
252 (Fig. 3).

253 The concentration of extractable P_o ranged from 38 to 91 $\text{mg}\cdot\text{kg}^{-1}$, which
254 accounted for 11–43% (27% average) of the extractable total P in the sediment. The
255 concentration of P_o fractions in the sediments decreased in the following order:
256 $\text{NaHCO}_3\text{-P}_o > \text{NaOH-P}_o > \text{HCl-P}_o > \text{H}_2\text{O-P}_o$ (Fig. 2b). $\text{H}_2\text{O-P}_o$ and $\text{NaHCO}_3\text{-P}_o$
257 accounted for 49–79% (61% average) and 13–64% (41% average) of the total $\text{H}_2\text{O-P}$
258 and $\text{NaHCO}_3\text{-P}$, respectively. Of the fulvic and humic acid-associated P as NaOH-P_o ,

259 the fulvic acid–combined P is considered to be comprised of moderately labile P_o ,
260 whereas humic acid–associated P is considered to be more resistant to biodegradation
261 (Zhang and Shan, 2008), and accounted for 8–52% (22% average) of total NaOH–P.
262 The HCl– P_o , representing moderately labile P_o in the sediment (Lü et al., 2016),
263 accounted for 2–49% (14% average) of the total HCl–P. These finding suggest that
264 there was more P_o presented as higher labile P species, which could easily release and
265 enter the overlying water to support algal growth. Compared with China’s five largest
266 freshwater lakes, Lake Erhai have stronger UV–radiation and higher microbial
267 activity because of higher altitude and warm and humid climatic conditions (Wang et
268 al., 2015). UV–radiation and microorganisms are important drivers in the degradation
269 of P_o release dissolved P_i through photochemical transformation and
270 biomineralization (Li et al., 2019). Therefore, the higher content of P_o in Lake Erhai
271 sediments than China’s five largest freshwater lakes (Fig. 3), indicating that Lake
272 Erhai sediment P_o might has greater potential to contribute internal P load.

273 3.2. Bioavailability of P_o

274 To further understand the bioavailability of P_o in the sediment, two kinds of
275 active P_o species (labile monoester and diester P) in the H_2O , $NaHCO_3$, NaOH, and
276 HCl fractions were hydrolyzed by APase and PDEase (Fig. 4). The concentration of
277 labile monoester P in H_2O – P_o ranged from 0.1 to 2.2 $mg\ kg^{-1}$, and accounted for
278 4.9–61.3% of H_2O – P_o , with an average concentration of 0.9 $mg\ kg^{-1}$ (24.7%).
279 Concentrations of labile monoester P in $NaHCO_3$ – P_o were 2.8–9.7 $mg\ kg^{-1}$ (6.5mg
280 kg^{-1} average), accounting for 9.7–38.6% (20.8% average) of $NaHCO_3$ – P_o . Labile

281 monoester P, i.e. 0.3–4.9 mg kg⁻¹ (1.6 mg kg⁻¹ average) and accounted for 1.7–24.2%
282 (11.1% average) of all NaOH-P_o. For HCl-P_o, concentrations of labile monoester P
283 were 0.7–3.6 mg kg⁻¹ (1.8 mg kg⁻¹ average), accounting for 5.9–62.5% (28.4%
284 average) of all HCl-P_o (Fig. 4a).

285 Diester P consisting of DNA (DNA-P), ribonucleic acids (RNA-P) and
286 phospholipids, is degraded more rapidly than monoester P (Makarov et al., 2002).
287 Amounts of diester P were 0.1–1.1 mg kg⁻¹ (average 0.6 mg kg⁻¹), and accounted for
288 4.3–29.4% (14.5% average) of H₂O-P_o. Corresponding values for the NaHCO₃-P_o
289 fraction were 1.9–10.6 mg kg⁻¹ (5.8–44.0%), with an average value of 5.5 mg kg⁻¹
290 (18.8%), and the values for the NaOH-P_o fraction were 1.8–9.6 mg kg⁻¹ (11.8–88.4%
291 average), with an average of 4.5 mg kg⁻¹ (32.9%). The amount of diester P in the
292 HCl-P_o fraction was 0.3–5.6 mg kg⁻¹ (5.2–62.4%), with average values of 1.7 mg kg⁻¹
293 (27.0%) in (Fig. 4b).

294 Contents of total P_o hydrolyzed by Apase and PDEase were in the decreasing
295 order of size, NaHCO₃-P_o > NaOH-P_o > HCl-P_o > H₂O-P_o. However, percentages of
296 hydrolyzed P_o in the P_o fractions were in decreasing order of size, HCl-P_o >
297 NaOH-P_o > H₂O-P_o > NaHCO₃-P_o, with average values of 56%, 43%, 40%, and
298 39%, respectively (Fig. 4c). Therefore, P_o fractions characterized by sequential
299 extraction and enzymatic hydrolysis in sediments from Lake Erhai could be classified
300 accordance with their decreasing bioavailability in order HCl-P_o > NaOH-P_o >
301 H₂O-P_o > NaHCO₃-P_o. In the traditional sequential P_o fractionation, H₂O-P_o and
302 NaHCO₃-P_o are considered to be labile P_o, while HCl-P_o and partly NaOH-P_o (fulvic

303 acid associated P_o) are moderately labile P_o (Ivanoff et al., 1998). However, this study
304 found that the percentages of hydrolyzed P_o in the HCl- P_o and NaOH- P_o were higher
305 than that of H₂O- P_o and NaHCO₃- P_o fractions in sediments. This suggested that
306 traditional sequential fractionation of P_o might overestimate the availability of labile
307 P_o in sediments. Overall, 21–66% (40% average) of the extractable P_o could be
308 hydrolyzed by APase and PDEase in Lake Erhai. The increase in alkaline phosphatase
309 during the period of algal growth could promote the degradation of bioavailable P_o ,
310 replenish available P pools in the overlying water and further facilitate algal growth.

311

312 3.3. Environmental process of bioavailable P_o

313 The pools of P_o in sediments are intrinsically linked with the amount and
314 structure of the deposited OM (Lü et al., 2016). This reflects that, the amount and
315 structure of OM might be key drivers that responsible for the biogeochemical cycle of
316 bioavailable P_o , thereby influence the distribution pattern of P_o in the sediments.

317 UV-visible has been used as an effective tool to characterise the structure of
318 dissolved organic matter (DOM) (Zhou et al., 2015). The spatial distribution of
319 UV-visible parameters such as the A_{253}/A_{203} , $SUVA_{260}$, $SUVA_{254}$, and E_2/E_3 of DOM
320 solutions within Lake Erhai are presented in Fig. 5a. $SUVA_{260}$ values can indicate the
321 concentration of hydrophilic substances, with higher values corresponding to more
322 hydrophobic substances (Jaffrain et al., 2007). $SUVA_{254}$ values are proxies for
323 estimating the concentration of aromatic in DOM, with higher $SUVA_{254}$ values
324 corresponding to higher degree of aromaticity and humification (Yeh et al., 2014;

325 [Weishaar et al., 2003](#)). Li et al (2014) found that higher A_{253}/A_{203} ratios corresponded
326 to higher concentrations of substitution groups (hydroxyl, carbonyl, carboxyl, and
327 ester groups). In this study, $SUVA_{260}$, $SUVA_{254}$ values, and A_{253}/A_{203} ratios increased
328 steadily from the northern to the southern sampling areas, indicating increasing
329 hydrophilic substances, substitution groups, aromaticity and humification in the DOM.
330 Variations in the E_2/E_3 ratios were related to differences in the humification level and
331 molecular weight of DOM, with lower E_2/E_3 ratios reflecting higher molecular weight
332 ([He et al., 2008](#); [Peuravouri and Pihlaja, 1997](#)). In Lake Erhai sediments, the E_2/E_3
333 ratios decreased steadily from the northern to southern areas, indicating that sediment
334 DOM has a higher molecular weight. The structure of the DOM in the sediments
335 became to more complex as you move from the northern to the southern part of Lake
336 Erhai. This fact can be inferred by two phenomena: (1) the deposition of OM in the
337 south experienced a longer period of degradation by UV-radiation due to the flow of
338 water from north to south ([Cory et al., 2015](#)), and (2) the relatively higher
339 humification of OM because of the somewhat higher microbial populations in the
340 southern areas due to domestic pollution (Fig. 5b).

341 The distribution of bioavailable P_o (as total hydrolyzable P_o) displayed a
342 decreasing content gradient from southern to northern sampling sites, with the mean
343 values of 26.1, 22.9, and 19.9 $mg\ kg^{-1}$ in the southern, middle and northern areas,
344 respectively (Fig. 6a). The correlation between bioavailable P_o and UV-radiation
345 parameters was not strong except E_2/E_3 ratio (Table 1). However, the more
346 substitution groups of aromatic rings, and higher molecular weights and humification

347 degree that DOM contains in the sediment, the higher content of bioavailable P_o will
348 be in the sediment (Fig. 6a). From the northern to the southern sampling areas,
349 sediment DOM contains more substitution groups and has higher degree of
350 humification and higher molecular weights ($SUVA_{254}$, A_{253}/A_{203} and E_2/E_3). The
351 substitution groups could potentially form stable compounds via adsorption and
352 complexation with nutrient, redox metal ions and organic pollutants (Li et al., 2014).
353 High humification degree could better sustain the release and conversion of the DOM
354 in sediment (Li et al., 2015). Furthermore, microorganisms have difficulty degrading
355 and utilizing organic molecules with high molecular weights and high degree of
356 aromaticity (He et al., 2011). Therefore, the degradation and release of bioavailable P_o
357 in sediments can be alleviated due to the stabler structure of DOM from the northern
358 to the southern in Lake Erhai.

359 Besides the structure and composition of DOM, phosphatase hydrolysis is
360 another factor that significantly affects the bioavailable P_o content (Hakulinen et al.,
361 2005). Large amounts of phytoplankton are believed to enhance the activation of
362 alkaline phosphatase (Sabine et al., 2005; Zhou et al., 2008). As a result, the sediment
363 bioavailable P_o would degrade and enter into the overlying water, because there is
364 abundant alkaline phosphatase during the algal growth period. In Lake Erhai, higher
365 chlorophyll *a* concentrations appeared in the northern region (Fig. 5b), which would
366 signal the greater production of alkaline phosphatase, thereby enhance the degradation
367 of bioavailable P_o in this region. The relatively low content of bioavailable P_o
368 (especially diester P) in the northern sites demonstrated that phytoplankton biomass is

369 also an important factor in determining the accumulation of bioavailable P_o in
370 sediments.

371 The bioavailable P_o components also displayed variability in their spatial
372 distribution. The diester P showed a similar trend as bioavailable P_o in the sediment,
373 with mean values of 14.2, 13.7, and 8.3 mg kg^{-1} in the southern, middle, and northern
374 areas, respectively (Fig. 6b). Diester P was positively correlated with A_{253}/A_{203} and
375 $SUVA_{254}$, with correlation coefficients of 0.567 ($p < 0.05$) and 0.587 ($p < 0.02$),
376 respectively. Diester P also had negative relationship with the E_2/E_3 ratio ($r = 0.772$, p
377 < 0.01) (Table 1), indicating that the more complex structure of DOM is in the
378 sediments, the higher content of diester P will be in the sediment. Furthermore, diester
379 P was negatively correlated with chlorophyll *a* concentration ($r = 0.489$, $p < 0.05$),
380 which could be attributed to the great degradation of diester P in the sediment because
381 of somewhat richer alkaline phosphatase in higher phytoplankton biomass. Sediment
382 labile monoester P was greatest in the southern (11.9 mg kg^{-1}) and northern (11.6 mg
383 kg^{-1}) areas and lowest in the middle region (9.1 mg kg^{-1}) (Fig. 6c). The correlation
384 was not strong between the content of labile monoester P and OM (Table 1), which
385 possibly showed that labile monoester P was active P_o species in the sediments. The
386 conversion of diester P is an important factor affecting labile monoester P distribution.
387 Ahlgren et al (2006) found that diester P that originated from microorganisms will be
388 degraded to phosphate or labile monoester P rapidly after microorganisms die. In the
389 northern of Lake Erhai, the diester P was degraded more easily than that of in
390 middle and southern areas, which might enhance labile monoester P accumulation in

391 the sediments. The higher content of labile monoester P in southern are likely related
392 to the stabler structure of DOM.

393

394 *3.4. Potential role of bioavailable P_o in algal growth*

395 The contribution of sediment P_o to algal growth was associated with
396 bioavailability and environmental conditions (Ni et al., 2016, 2019). In Lake Erhai,
397 bioavailable P_o accounted for 21–66% of extractable P_o and 4–17% of extractable
398 total P in the sediments. Enzymatic hydrolysis is the most important driver of P_o
399 release from sediments (Hakulinen et al., 2005), and APase and PDEase are
400 widespread in Lake Erhai (Wang et al., 2015). During the periods of algal growth
401 (August to October), as phytoplankton biomass increases, activities of APase and
402 PDEase would also increase in the sediment, which especially obvious during the
403 period of potential algal blooms (Zhou et al., 2002; Xu, 2005). Therefore, the large
404 accumulation of bioavailable P_o allows for possible degradation that would replenish
405 the available P at the sediment–water interface, and further support algal growth. This
406 could be the reason why Lake Erhai nutrients are very low, but its phytoplankton
407 biomass always maintains a high level, and outbreak blooms occur frequently. In turn,
408 Death and sedimentation of phytoplankton enhanced the accumulation of P_o and OM
409 in the sediments. Sediments OM was primarily derived from autochthonous sources
410 based on the results of TOC /TN ratio (5.6–11.8, 9.2 averages) (Fig. 5b). Meyers and
411 Ishiwatari, (1993) reported that the TOC /TN ration for vascular land plants is usually
412 greater than 20, whereas plankton and bacteria have a TOC / TN ratio of between 4

413 and 10. Therefore, the high phytoplankton biomass and blooming phenomena in Lake
414 Erhai would likely persist indefinitely without an intervention to interrupt the supply
415 cycle of P_o from the sediments (Fig. 7).

416 Taken with the results presented in section 3.3, these results indicate that the
417 accumulation and release of bioavailable P_o are related to the structural of DOM. The
418 overlying water of Lake Erhai is constantly exposed to strong UV-B radiation
419 because of its high altitude (1974 m), which leads to a high degree of DOM
420 humification in the sediment (Ni et al., 2019). As a result, bioavailable P_o released
421 from the sediment could be inhibited due to the shielding action of the high degree of
422 DOM humification. Compared with the southern and middle regions of Lake Erhai,
423 the humification degree of DOM in northern region is lower (Fig. 5), indicating the
424 greater potential risk of bioavailable P_o release in this region. Furthermore, gradual
425 increases in the number of microorganisms and phytoplankton (Zhang et al., 2015;
426 Wang et al., 2015) might increase the degradation rate of bioavailable P_o from
427 sediment via the enzymatic hydrolysis. Therefore, reducing internal sediment P_o
428 accumulation, controlling sediment P_o degradation and release, strengthening algal
429 removal, improving microbial habitats, optimizing key environmental conditions,
430 and human intervention in the biogeochemical cycle of bioavailable P_o are important
431 aspects to consider in the management and control of the algal blooms in Lake Erhai.

432

433 **4. Conclusions**

434 We investigated the importance of P_o to internal P loads in Lake Erhai. Our

435 results showed that extractable P_o accounted for 11%–43% (27% average) of
436 extractable total P, and bioavailable P_o accounted for 21–66% (40%) of extractable P_o
437 in the sediments. The massive storage of bioavailable P_o represents an important form
438 of available P, essential to internal loads. The bioavailable P_o includes mainly labile
439 monoester P and diester P was identified in the sequential extractions by H_2O ,
440 $NaHCO_3$, $NaOH$, and HCl . 40% of H_2O-P_o , 39% of $NaHCO_3-P_o$, 43% of $NaOH-P_o$,
441 and 56% of $HCl-P_o$ can be hydrolyzed to labile monoester and diester P, suggesting
442 that the bioavailability of P_o fractions was in decreasing order as follows: $HCl-P_o >$
443 $NaOH-P_o > H_2O-P_o > NaHCO_3-P_o$. It is implied that traditional sequential
444 fractionation of P_o might overestimate the availability of labile P_o in sediments.

445 We also examined the environmental processes of bioavailable P_o and its
446 potential role in algal growth. The results showed that the stabler structure of DOM
447 alleviated the degradation and release of diester P, abundant alkaline phosphatase due
448 to higher algal biomass promoted the degradation of diester P. The stability of DOM
449 structure and the degradation of diester P might responsible for the spatial differences
450 of labile monoester P. The biogeochemical cycle of bioavailable P_o could replenish
451 available P pools in overlying water and facilitate algal growth.

452

453 **Conflict of interest**

454 The authors declare that they have no conflict of interests.

455

456 **Acknowledgements**

457 This research was jointly supported by the National High-level Personnel of
458 Special Support Program (People Plan, grant number 312232102) and the Open-End
459 fund of the Kunming China International Research Center for Plateau-Lake (grant
460 number 230200069).

461

462 **References**

- 463 Ahlgren, J., Tranvik, L., Gogoll, A., Waldeback, M., Markides, K., Rydin, E., 2005.
464 Sediment depth attenuation of biogenic phosphorus compounds measured by ³¹P
465 NMR. *Environ. Sci. Technol.* 39, 867–872.
- 466 Bai, X.L., Ding, S.M., Fan, C.X., Liu, T., Shi, D., Zhang, L., 2009. Organic
467 phosphorus species in surface sediments of a large, shallow, eutrophic lake, Lake
468 Taihu, China. *Environ. Pollut.* 157, 2507–2513.
- 469 Baldwin, D.S., 2013. Organic phosphorus in the aquatic environment. *Environ. Chem.*
470 10, 439–454.
- 471 Bünemann, E. K., 2008. Enzyme additions as a tool to assess the potential
472 bioavailability of organically bound nutrients. *Soil Biol. Biochem.* 40(9),
473 2116–2129.
- 474 Chen, M.S., Ding, S.M., Chen, X., Sun, Q., Fan, X.F., Lin, J., Ren, M.Y., Yang, L.Y.,
475 Zhang, C.S., 2018. Mechanisms driving phosphorus release during algal blooms
476 based on hourly changes in iron and phosphorus concentrations in sediments.
477 *Water Res.* 133, 153–164.
- 478 Copetti, D.G., Tartari, G., Valsecchi, I., Salerno, F., Viviano, G., Mastroianni, D., Yin,

479 H., Viganò, L., 2019. Phosphorus content in a deep river sediment core as a
480 tracer of long-term (1962–2011) anthropogenic impacts: A lesson from the
481 Milan metropolitan area. *Sci. Total. Environ.* 646:37–48.

482 Cory, R.M., Harrold, K.H., Neilson, B.T., Kling, G. W., 2015. Controls on dissolved
483 organic matter (DOM) degradation in a headwater stream: the influence of
484 photochemical and hydrological conditions in determining light-limitation or
485 substrate-limitation of photo-degradation. *Biogeosciences* 12(22), 6669–6685.

486 Ding, S.M., Han, C., Wang, Y.P., Yao, L., Wang, Y., Xu, D., Sun, Q., Williams, P.N.,
487 Zhang, C.S., 2015. In situ, high-resolution imaging of labile phosphorus in
488 sediments of a large eutrophic lake. *Water Res.* 74, 100–109.

489 Fan, C.X., Zhang, L., Bao, X.M., You, B.S., Zhong, J.J., Wang, J.J, Ding, S.M., 2006.
490 Mobile mechanism of biogenic elements and their quantification on the
491 sediment-water interface of Lake Taihu: II. Chemical thermodynamic mechanism
492 of phosphorus release and its source-sink transition. *J. Lake. Sci.* 18 (3), 207–217
493 (in Chinese).

494 Hakulinen, R., Kähkönen, M.A., Salkinija-Salonen, M.S., 2005. Vertical distribution
495 of sediment enzyme activities involved in the cycling of carbon, nitrogen,
496 phosphorus and sulphur in three boreal rural lakes. *Water Res.* 39(1), 2319–2326.

497 He, X.S., Xi, B.D., Wei, Z., Guo, X., Li, M., An, D., Liu, H., 2011. Spectroscopic
498 characterization of water extractable organic matter during composting of
499 municipal solid waste. *Chemosphere* 82, 541–548.

500 He, Z., Griffin, T.S., Honeycutt, C.W., 2004. Enzymatic hydrolysis of organic

501 phosphorus in swine manure and soil. *J. Environ. Qual.* 33, 367–372.

502 Huang, B.Q., Ou, L.J., Hong, H.S., Luo, H.W., Wang, D.Z., 2005. Bioavailability of
503 dissolved organic phosphorus compounds to typical harmful dinoflagellate
504 *prorocentrum donghaiense* lu *Mar. Pollut. Bulle.* 51, 838–844.

505 Huo, S.L., Li, Q.Q., Zan, F.Y., Xi, B.D., Liu, Q.X., 2011. Characteristics of organic
506 phosphorus fractions in different trophic sediments of lakes, China. *Environ. Sci.*
507 32(4), 1000–1007 (in Chinese).

508 Jaffrain, J., Gerard, F., Meyer, M., 2007. Assessing the quality of dissolved organic
509 matter in forest soils using ultraviolet absorption spectrophotometry. *Soil. Sci.*
510 *Society. America. J.* 71(6), 1851–1858.

511 Ji, N.N., Wang, S.R., Zhang, L., 2017. Characteristics of dissolved organic
512 phosphorus inputs to freshwater lakes: A case study of Lake Erhai, southwest
513 China. *Sci. Total. Environ.* 601–602, 1544–1555.

514 Jin, X.C., Pang, Y., Wang, S.R., Zhou, X.N., 2008. Phosphorus forms and its
515 distribution character in sediment of shallow lakes in the Middle and Lower
516 Reaches of the Yangtze River. *J. Agro-Environ. Sci.* 27(1), 0279–0285 (in
517 Chinese).

518 Jin, X.C., Wang, S.R., Pang, Y., Wu, F.C., 2006. Phosphorus fractions and the effect of
519 pH on the phosphorus release of the sediments from different trophic areas in
520 Taihu Lake, China. *Environ. Pollut.* 139, 288–295.

521 Kim, L., Choi, E., Stenstrom, M.K., 2003. Sediment characteristics, phosphorus types
522 and phosphorus release rates between river and lake sediments. *Chemosphere* 50,

523 53–61.

524 Lei, P., Zhang, H., Wang, C., Pan, K., 2018. Migration and diffusion for pollutants
525 across the sediment-water interfere in lake: A review. *J. Lake. Sci.* 30(6),
526 1489–1508 (in Chinese).

527 Li, X.L., Guo, M.L., Duan, X.D., Zhao, J.W., Hua, Y.M., Zhou, Y.Y., Liu, G.L.,
528 Dionysiou, D.D., 2019. *Environ. Inter.* 130, 104916.

529 Li, Y.P., Wang, S.R., Zhang, L., 2015. Composition, source characteristic and
530 indication of eutrophication of dissolved organic matter in the sediments of Erhai
531 Lake. *Environ. Earth. Sci.* 74, 3739–3751.

532 Li, Y.P., Wang, S.R., Zhang, L., Zhao, H.C., Jiao, L.X., Zhao, Y.L., He, X.S., 2014.
533 Composition and spectroscopic characteristics of dissolved organic matter
534 extracted from the sediment of Erhai Lake in China. *J. Soils. Sediments.* 14,
535 1599–1611.

536 Liao, J.Y., Wang, S.R., Yang, S.W, Chu, Z.S., Jin, X.C., Zhang, Y., Zeng, Q.R., 2010.
537 Characteristics of organic phosphorus in different forms of lake sediments from
538 east plain region. *Environ. Sci. Res.* 23(9), 1142–1150 (in Chinese).

539 Liu, W.B., Wang, S.R., Zhang, L., Ni, Z.K., Zhao, H.C., Jiao, L.X., 2015.
540 Phosphorus release characteristics of sediments in Erhai Lake and their impact
541 on water quality, China. *Environ. Earth. Sci.* 74(5): 3753–3766.

542 Lorenzen, C.J., 1967. Determination of chlorophyll and phaeo-pigments:
543 spectrophotometric equations. *Limnol. Oceanogr.* 12(2), 343–346.

544 Lü, C.W., Wang, B., He, B., Volf, R.D., Zhou, B., Guan, R., Zuo, L., Wang, W.Y., Xie,

545 Z.L., Wang, J.H., Yan, D.H., 2016. Responses of organic phosphorus fractionation
546 to environmental conditions and lake evolution. *Environ. Sci. Technol.* (50),
547 5007–5016.

548 Makarov, M., Haumaier, L., Zech, W., 2002. Nature of soil organic phosphorus: An
549 assessment of peak assignments in the diester region of ^{31}P NMR spectra. *Soil*
550 *Biol. Biochem.* 34, 1467–1477.

551 Mandal, S., Goswami, A.R., Mukhopadhyay, S.K., Ray, S., 2015. Simulation model of
552 phosphorus dynamics of an eutrophic impoundment—East Calcutta Wetlands, a
553 Ramsar site in India. *Ecol. Model.* 306, 226–239.

554 Meyers, P.A., Ishiwatari, R., 1993. Lacustrine organic geochemistry – an overview of
555 indicators of organic matter sources and diagenesis in lake sediments. *Org.*
556 *Geochem.* 20, 867–900.

557 Monbet, P., McKelvie, I.D., Saefumillah, A., Worsfold, P.J., 2007. A protocol to assess
558 the enzymatic release of dissolved organic phosphorus species in waters under
559 environmentally relevant conditions. *Environ. Sci. Technol.* 41 (21), 7479–7485.

560 Nanjing Institute of Soil, Chinese Academy of Science, 1978. Soil and physical
561 chemistry analysis. Shanghai Technology Press, Shanghai (in Chinese).

562 Ngatia, L.W., Hsieh, Y.P., Nemours, D., Fu, R., Taylor, R.W., 2017. Potential
563 phosphorus eutrophication mitigation strategy: Biochar carbon composition,
564 thermal stability and pH influence phosphorus sorption. *Chemosphere* 180,
565 201–211.

566 Ni, Z.K., Wang, S.R., 2015. Historical accumulation and environmental risk of

567 nitrogen and phosphorus in sediments of Erhai Lake, Southwest China. *Ecol.*
568 *Engine.* 79, 42–53.

569 Ni, Z.K., Wang, S.R., Wang, Y.M., 2016. Characteristics of bioavailable organic
570 phosphorus in sediment and its contribution to lake eutrophication in China.
571 *Environ. Pollut.* 219, 537–544.

572 Ni, Z.K., Wang, S.R., Zhang, B.T., Wang, Y.M., Li, H., 2019. Response of sediment
573 organic phosphorus composition to lake trophic status in China. *Sci. Total.*
574 *Environ.* 652, 495–504.

575 OECD. 1982. *Eutrophication of Waters-monitoring, Assessment and Control*; Paris,
576 France: Organization for Economic Co-operation and Development.

577 Ruban, V., López-Sánchez, J.F., Pardo, P., 1999. Selection and evaluation of
578 sequential extraction procedures for the determination of phosphorus forms in
579 lake sediment. *J. Environ. Monitor.* (1), 51–56.

580 Sabine, W., Helmut, F., Matrtin, P.T., 2005. Regulation and seasonal dynamics of
581 extracellular enzyme activities in the sediments of a large lowland river. *Micro.*
582 *Ecol.* 50, 253–267.

583 Shinohara, R., Hiroki, M., Kohzu1, A., Imai, A., Inoue, T., 2017. Role of organic
584 phosphorus in sediment in a shallow eutrophic lake. *Water. Resour. Res.* 53,
585 7175–7189.

586 Sun, J., Wang, S.R., Zeng, Q.R., Jiao, L.X., Jin, X.C., Yang, S.W., 2010. Distribution
587 characteristics of organic phosphorus fractions and influencing factors in surface
588 sediments of Lake Erhai. *Res. Environ. Sci.* 24(11), 1226–1232 (in Chinese).

589 Ting, D.S., Appan, A., 1996. General characteristics and fractions of P in aquatic
590 sediments of two tropical reservoirs. *Water. Sci. Technol.* 34, 53–59.

591 Wang, S.R., Zhao, H.C., Chu, Z.S., Jiao, L.X., Zhang, L., Ni, Z.K., 2015.
592 Eutrophication process and mechanism of Erhai Lake. Science Press, Beijing (in
593 Chinese).

594 Wang, Z.C., Huang, S., Li, D.H., 2019. Decomposition of cyanobacterial bloom
595 contributes to the formation and distribution of iron-bound phosphorus (Fe-P):
596 Insight for cycling mechanism of internal phosphorus loading. *Sci. Total.*
597 *Environ.* 652, 696–708.

598 Weishaar, J.L., Aiken, G.R., Bergamaschi, B.A., Fram, M.S., Fujii, R., Mopper, K.,
599 2003. Evaluation of specific ultraviolet absorbance as an indicator of the
600 chemical composition and reactivity of dissolved organic carbon. *Environ. Sci.*
601 *Technol.* 37, 4702–4708.

602 Worsfold, P.J., Monbet, P., Tappin, A.D., Fitzsimons, M.F., Stiles, D.A., Mckelvie,
603 I.D., 2008. Characterisation and quantification of organic phosphorus and
604 organic nitrogen components in aquatic systems: a review. *Anal. Chim. Acta.* 624
605 (1), 37–58.

606 Xu, Y.T., 2005. The study on the effect of bacteria on organic phosphorus cycling in
607 sediment of Xihu Lake. Zhejiang University Press, Hangzhou (in Chinese).

608 Yeh, Y.L., Yeh, K.J., Hsu, L.F., Yu, W.C., Lee, M.H., Chen, T.C., 2014. Use of
609 fluorescence quenching method to measure sorption constants of phenol. *J.*
610 *Hazard. Mater.* 277, 27–33.

611 Yue, T., Zhang, D.L., Hu, C.X., 2014. Utilization of phosphorus in four forms of the
612 three dominant microcystis morphospecies in Lake Taihu. *J. Lake Sci.* 26(3),
613 379–384 (in Chinese).

614 Zhang, H., Shan, B.Q., 2008. Historical distribution and partitioning of phosphorus in
615 sediments in an agricultural watershed in the Yangtze–Huaihe region, China.
616 *Environ. Sci. Technol.* 42, 2328–2333.

617 Zhang, L., Fan, C.X., Wang, J.J., Chen, Y.W., Jiang, J.H., 2008. Nitrogen and
618 phosphorus forms and release risks of lake sediments from the middle and lower
619 reaches of the Yangtze River. *J. Lake. Sci.* 20 (3), 263–270 (in Chinese).

620 Zhang, L., Wang, S.R., Li, Y.P., Zhao, H.C., Qian, W.B., 2015. Spatial and temporal
621 distributions of microorganisms and their role in the evolution of Erhai Lake
622 eutrophication. *Environ. Earth. Sci.* 74, 3887–3896.

623 Zhao, H.C., Wang, S.R., Jiao, L.X., Yang, S.W., Liu, W.B., 2013. Characteristics of
624 temporal and spatial distribution of different forms of phosphorus in the
625 sediments of Erhai Lake. *Res. Environ. Sci.* 26(3), 227–234 (in Chinese).

626 Zhou, M.H., Meng, F.G., 2015. Using UV–vis absorbance spectral parameters to
627 characterize the fouling propensity of humic substances during ultrafiltration.
628 *Water Res.* 87, 311–319.

629 Zhou, Q.X., Gibson, C.E., Zhu, Y.M., 2001. Evaluation of phosphorus bioavailability
630 in sediments of three contrasting lakes in China and the UK. *Chemosphere* 42(2),
631 221–225.

632 Zhou, Y.Y., Li, J. Q., Zhang, M., 2002. Temporal and spatial variations in kinetics of

633 alkaline phosphatase in sediments of a shallow Chinese eutrophic lake (Lake
634 Donghu). *Water Res.* 36(8), 2084–2090.

635 Zhou, Y.Y., Song, C.L., Cao, X.Y., Li, J.Q., Chen, G.Y., Xia, Z.Y., Jiang, P.H., 2008.
636 Phosphorus fractions and alkaline phosphatase activity in sediments of a large
637 eutrophic Chinese lake (Lake Taihu). *Hydrobio* 599(1), 119–125.

638 Zhu, Y.R., Wu, F.C., He, Z.Q., Guo, J.Y., Qu, X.X., Xie, F.Z., Giesy, J.P., Liao, H.Q.,
639 Guo, F., 2013. Characterization of organic phosphorus in lake sediments by
640 sequential fractionation and enzymatic hydrolysis. *Environ. Sci. Technol.* 47,
641 7679–7687.

Figures:

Fig. 1. Location of Lake Erhai in China showing sampling sites in the northern (N1, N2, N3 and N4), middle (M1, M2, M3, M4 and M5), and southern (S1, S2, S3, S4 and S5) parts of the lake.

Fig. 2. Amount and percentage of P_i (a) and P_o (b) in H_2O , $NaHCO_3$, $NaOH$, and HCl fractions of total phosphorus, respectively.

Fig. 3. Comparison of release flux of soluble reactive phosphorus (SRP) and P_o contents of Lake Erhai and China's five largest freshwater lakes.

Fig. 4. Content (a) and relative abundance (b) of labile monoester P and diester P characterized by phosphatase in the H_2O , $NaHCO_3$, and $NaOH$ fractions, respectively.

Fig. 5. Spatial distributions of UV–visible parameters (A_{253}/A_{203} , $SUVA_{260}$, $SUVA_{254}$, and E_2/E_3) (a), OM, TOC / TN ratio, total microbial population, and Chlorophyll *a* (b) in Lake Erhai.

Fig. 6. Spatial distribution of total hydrolyzable P_o (a), diester P (b), and labile monoester P (c) hydrolyzed by enzymes (APase and PDEase) in the H_2O , $NaHCO_3$, $NaOH$, and HCl fractions in Lake Erhai sediments.

Fig. 7. Biogeochemical cycle of sediment P_o and the supply model of bioavailable P_o to algal growth in Lake Erhai.

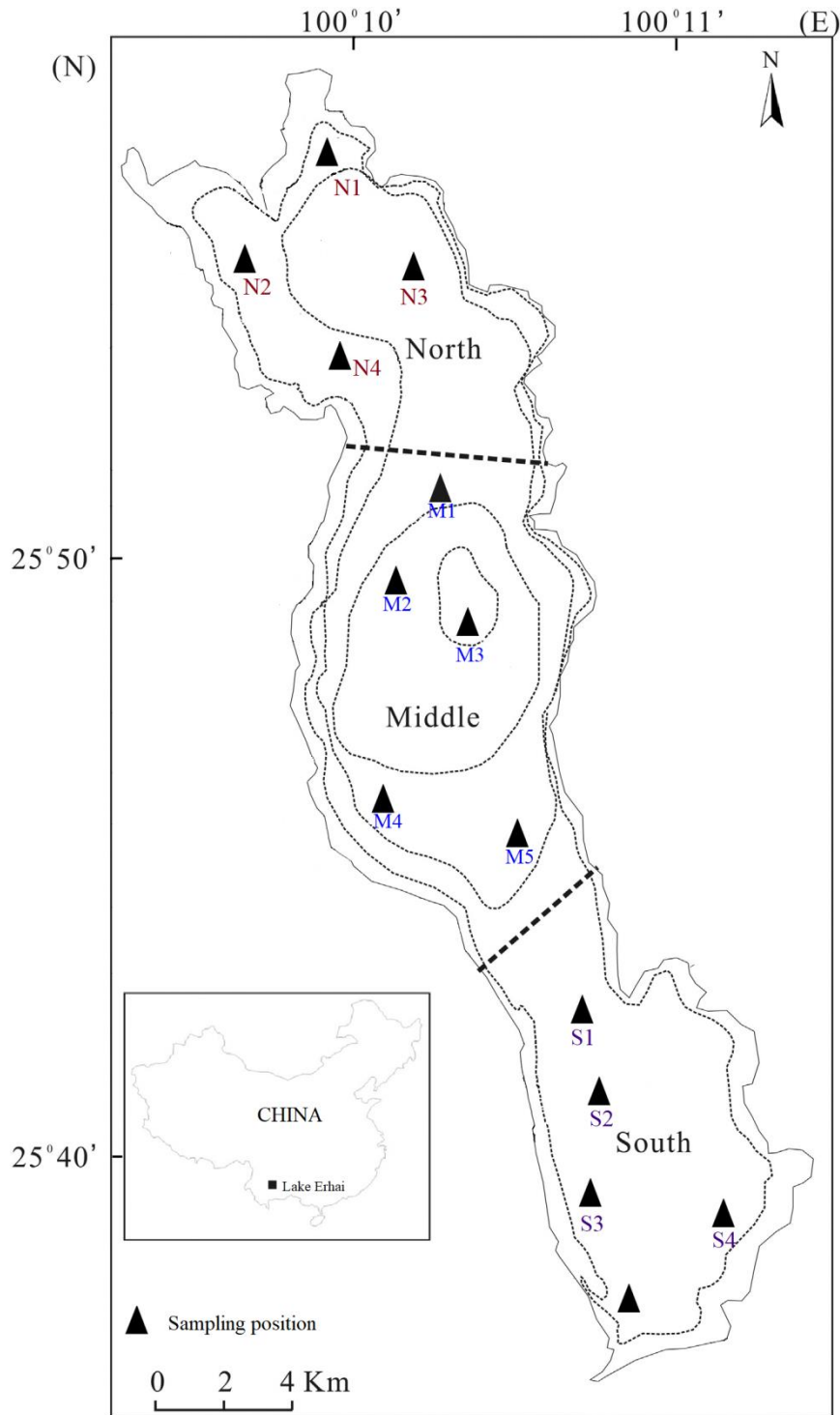


Fig. 1. Location of Lake Erhai in China showing sampling sites in the northern (N1, N2, N3 and N4), middle (M1, M2, M3, M4 and M5), and southern (S1, S2, S3, S4 and S5) parts of the lake.

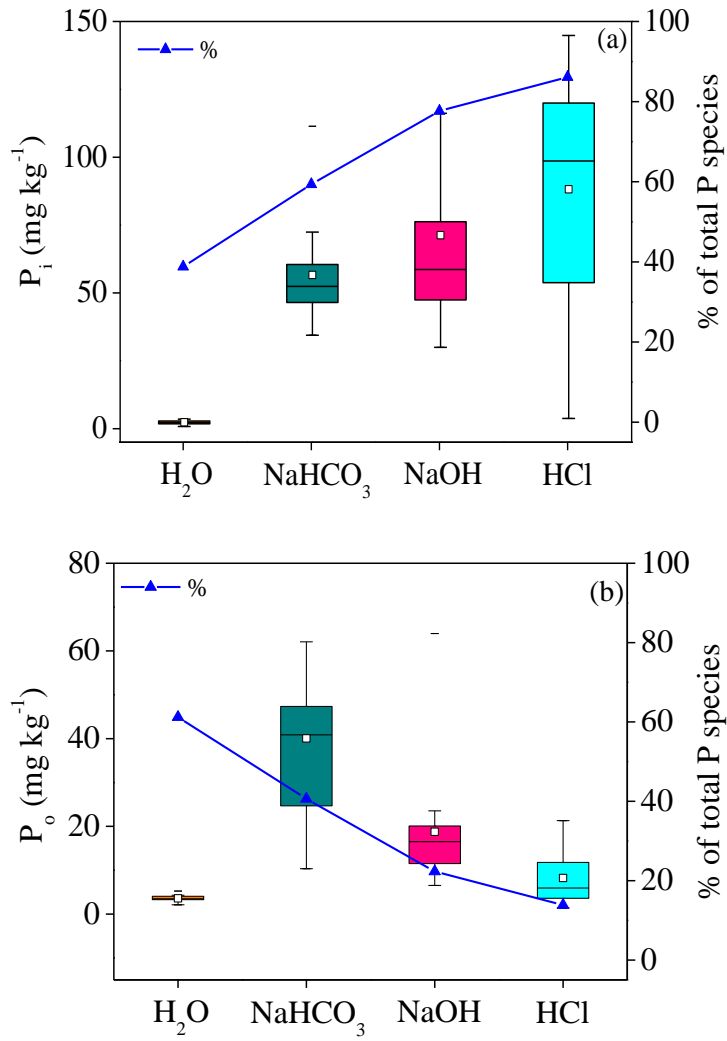


Fig. 2. Amount and mean percentage of P_i (a) and P_o (b) in H₂O, NaHCO₃, NaOH, and HCl fractions of total phosphorus, respectively. The box and whisker plots show the mean (square), median (horizontal line), 25th and 75th percentile (lower and upper edge of box), and the 5th and 95th percentile (lower and upper whisker).

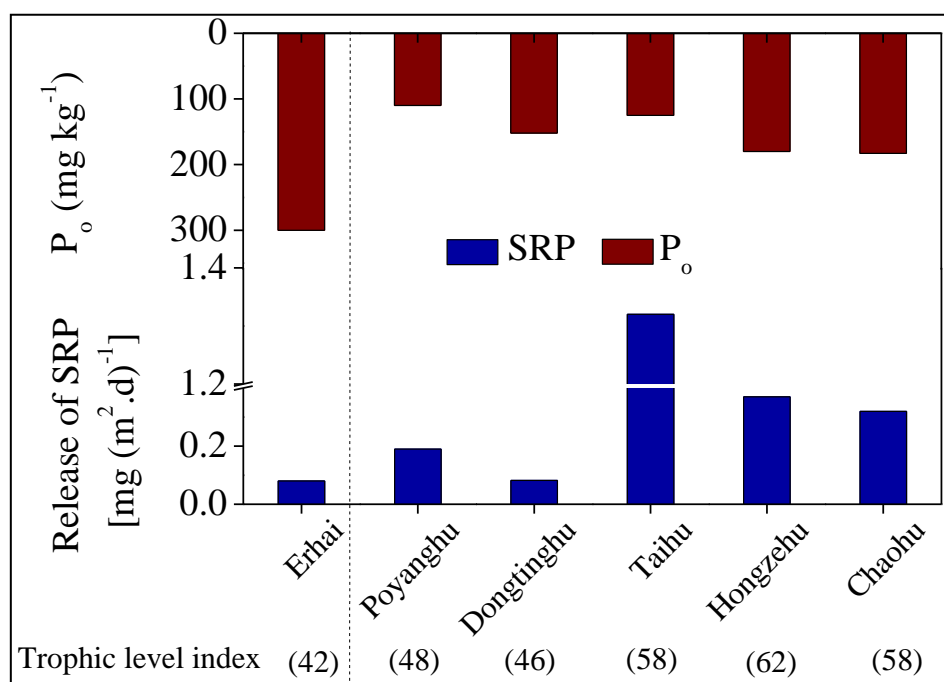


Fig. 3. Comparison of release flux of soluble reactive phosphorus (SRP) and P_o contents of Lake Erhai and China's five largest freshwater lakes. Shown are Lake Poyang (located in Jiangxi Province, with a surface area of 2,933 km²), Lake Dongting (located in Hunan Province, with a surface area of 18,000 km²), Lake Taihu (located in Jiangsu Province, with a surface area of 3,100 km²), Lake Hongze (located in Jiangsu Province, with a surface area of 2,069 km²), Lake Chao (located in Anhui Province, with an area of 753 km²). Data source: Fan et al., 2006, Zhang et al., 2008, Wang et al., 2015, Sun et al., 2011, Liao et al., 2010, Huo et al., 2011, Jin, et al., 2008.

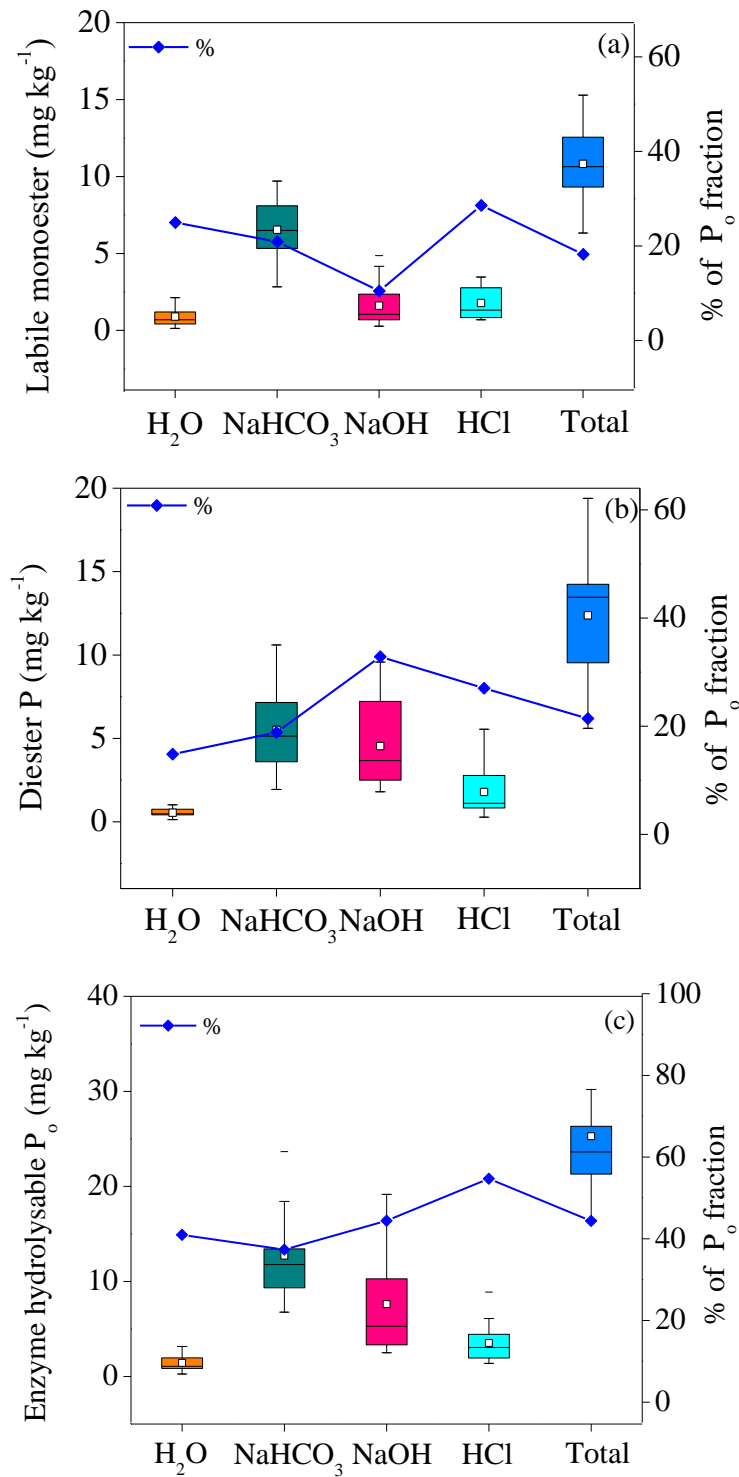


Fig.4. Content and relative abundance of labile monoester P and diester P characterized by phosphatase in the H₂O, NaHCO₃, and NaOH fractions, respectively. The box and whisker plots show the mean (square), median (horizontal line), 25th and 75th percentile (lower and upper edge of box), and the 5th and 95th percentile (lower and upper whisker).

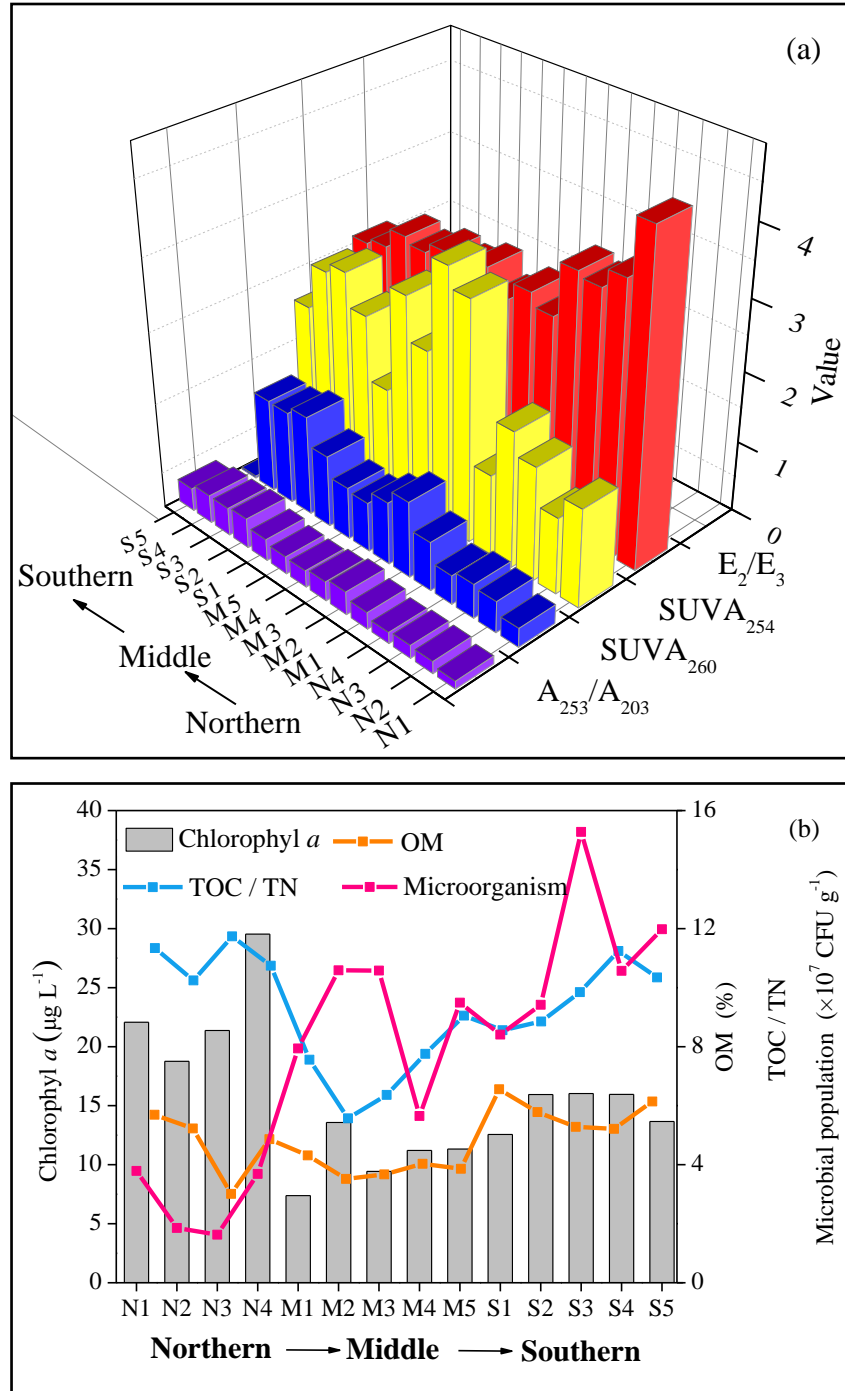


Fig. 5. Spatial distributions of UV–visible parameters (A_{253}/A_{203} , $SUVA_{260}$, $SUVA_{254}$, and E_2/E_3) (a), OM, TOC / TN ratio, total microbial population, and Chlorophyll *a* (b) in Lake Erhai.

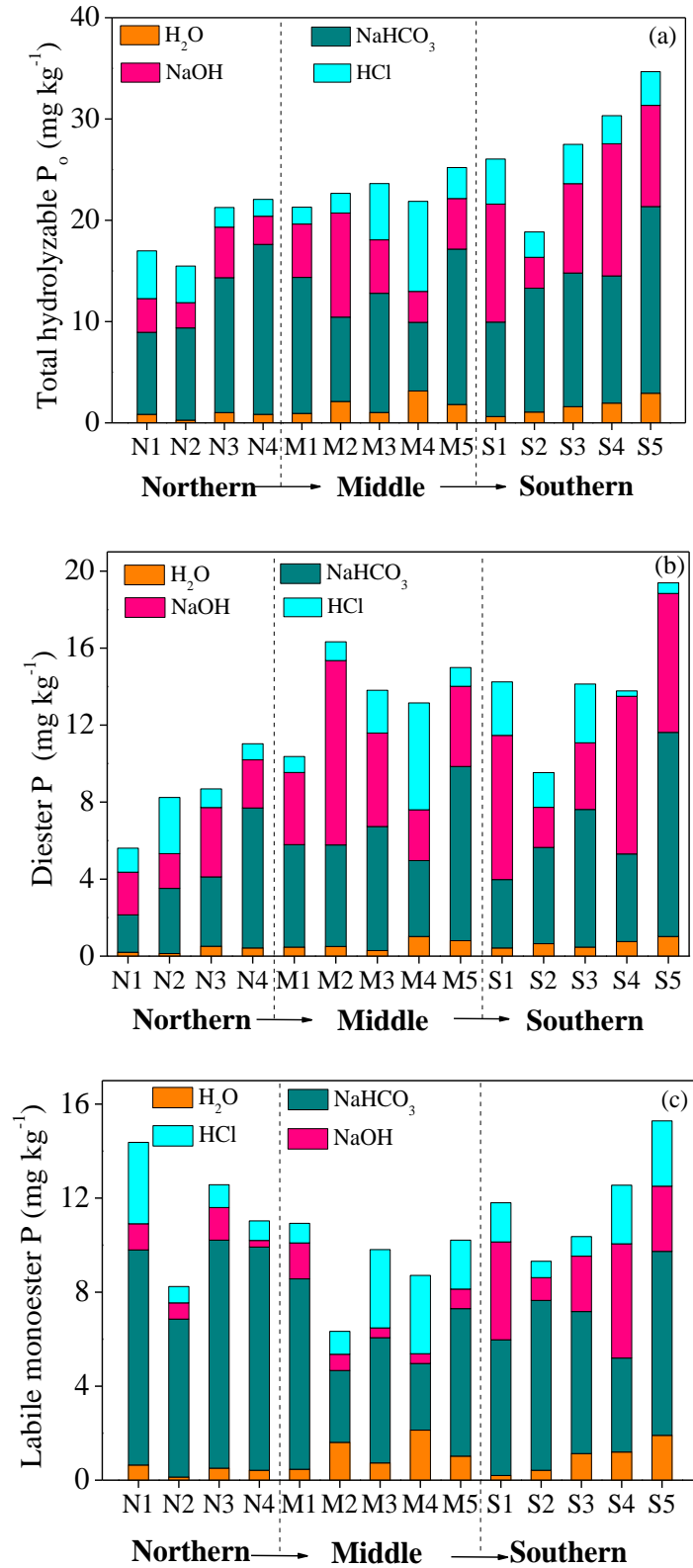


Fig. 6. Spatial distribution of total hydrolyzable P_0 (a), diester P (b), and labile monoester P (c) hydrolyzed by enzymes (APase and PDEase) in the H_2O , NaHCO_3 , NaOH , and HCl fractions in Lake Erhai sediments.

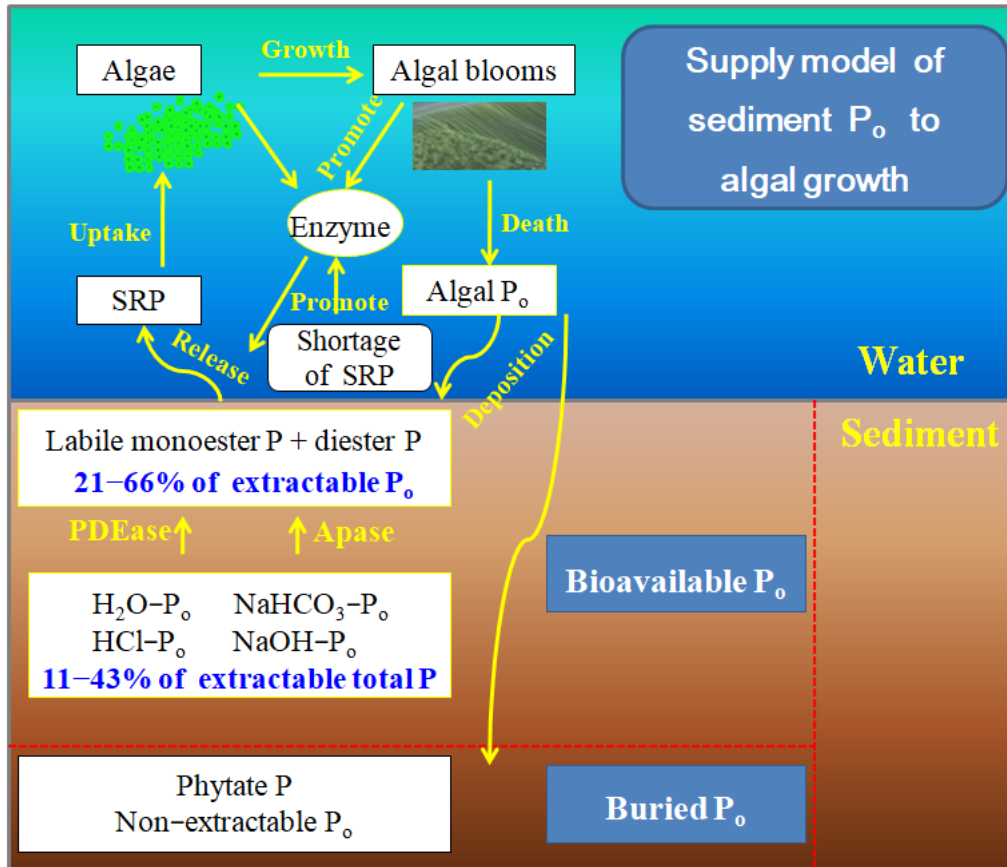


Fig. 7. Biogeochemical cycle of sediment P_0 and the supply model of bioavailable P_0

to algal growth in Lake Erhai.